Experimental study on the quasi-steady approximation of glottal flows

Takuto Honda,[1] Mayuka Kanaya,[1] Isao T. Tokuda,[1,a] (iD) Anne Bouvet,[2] Annemie Van Hirtum,[2] (iD) and Xavier Pelorson[2]

[1]*Graduate School of Science and Engineering, Ritsumeikan University, Noji–higashi, Kusatsu, Shiga 525–8577, Japan*

[2]*LEGI, UMR CNRS 5519, Grenoble Alpes University, France*

ABSTRACT:

To examine the quasi-steady approximation of the glottal flow, widely used in the modeling of vocal fold oscillations, intraglottal pressure distributions were measured in a scaled-up static vocal fold model under time-varying flow conditions. The left and right vocal folds were slightly open and set to a symmetric and oblique configuration with a divergence angle. To realize time-varying flow conditions, the flow rate was sinusoidally modulated with a frequency of 2 and 10 Hz, which correspond to 112.5 and 562.5 Hz, respectively, in real life. Measurements of the intraglottal pressures under both steady and time-varying flows revealed that the pressure profiles of the time-varying flow conditions are non-distinguishable from those of the steady flow conditions as far as they have the same subglottal pressure as an input pressure. The air-jet separation point was also non-distinguishable between the steady and the time-varying flow conditions. Our study therefore suggests that the time-varying glottal flow can be approximated as a series of steady flow states with a matching subglottal pressure in the range of normal vocalization frequencies. Since the glottal closure was not taken into account in the present experiment, our argument is valid except for such a critical situation. © *2022 Acoustical Society of America.* https://doi.org/10.1121/10.0010451

I. INTRODUCTION

In voice production, the vocal folds play a central role in generating the source sound. As an air-flow expelled from the lungs passes through the glottis, the glottal pressure acts as a driving force to induce self-sustained oscillations of the vocal folds. One of the most common assumptions made in the modeling and analysis of the glottal air-flow is the quasi-steady approximation, in which the glottal flow through the time-varying vocal folds is assumed to be the same as a sequence of steady flows through static vocal folds acting as a slowly-varying boundary condition. Following Krane *et al.* (2010), we define "quasi-steady flow" as a time-varying flow, for which time variations play a negligible role in determing the intraglottal pressure. "Unsteady flow," on the other hand, is defined as a time-varying flow, in which the time variations do affect the intraglottal pressure. Since the quasi-steady approximation simplifies the modeling of the glottal flow and consequently reduces its computational cost, it has been widely employed in the mathematical modeling of the vocal fold oscillations (Ishizaka and Flanagan, 1972; Pelorson *et al.*, 1994; Steinecke and Herzel, 1995; Titze, 2000; Titze and Alipour, 2006). An important question is whether the quasi-steady approximation of the glottal air-flow is valid in reality.

To examine the quasi-steadiness of the glottal flow, acoustic and aerodynamic measurements have been performed using a physical model of the oscillating vocal folds.

Mongeau *et al.* (1997), Zhang *et al.* (2002), and Deverge *et al.* (2003) reported that the quasi-steady flow assumption is applicable to predict the glottal aerodynamics for various vocal fold movements. Vilain *et al.* (2004) showed that quasi-steady boundary layer theory fits to the experiment well except during the vocal fold collision, in which unsteady or viscous terms become predominant. Kucinschi *et al.* (2006) showed that the glottal flow and the transglottal pressure were affected by the oscillation frequency of the vocal folds. Krane *et al.* (2010) showed that the phonatory flow can be assumed quasi-steady, except the final stages of the phonation cycle, during which the effect of convective and unsteady accelerations become non-negligible. Ringenberg *et al.* (2021) showed that cycle-to-cycle variations, e.g., jet switching and modulation, are inherent in the glottal flows. Numerical simulations have been also carried out to support the experimental studies (Alipour and Scherer, 2004; Kucinschi *et al.*, 2006).

Unsteady nature of the glottal pressure was also studied by an experimental set-up using a static vocal fold model and a time-varying flow. Hofmans *et al.* (2003) studied a time-varying flow passing through a rigid vocal fold model and reported that a boundary-layer model is effective for predicting the pressure drop inside the glottis. Vilain *et al.* (2004) showed that a quasi-steady boundary layer theory fits well with the experimental data measured under time-varying flow passing through a fixed vocal fold model. Although these studies suggested that the quasi-steady flow approximation is valid to describe the effect of time-varying

---

a)Electronic mail: isao@fc.ritsumei.ac.jp

glottal flow, they have monitored the glottal pressures only at a few points, which hardly provide a detailed pressure profile inside the glottis.

Measurement of the detailed pressure profile reveals important flow information such as the air-jet separation point. It has been considered that the moving separation point is essential for the vocal fold oscillations (Pelorson *et al.*, 1994). During the opening phase of the glottis, the vocal folds form a convergent shape, which moves the separation point superiorly to increase the glottal pressure. During the closing phase, on the other hand, the vocal folds form a divergent shape, which moves the separation point inferiorly to decrease the glottal pressure. To validate such change in the intraglottal pressure, detailed pressure distributions have been measured inside static physical models of the vocal folds under steady-flow conditions (Li *et al.*, 2006; Scherer *et al.*, 2001, 2002; Scherer *et al.*, 2010). It has been shown that the separation point is influenced by the flow rate and the glottal shapes. Such detailed pressure measurement along a static vocal fold model, however, has yet to be combined with a time-varying flow experiment.

The aim of the present study is to measure a detailed glottal pressure distribution under a time-varying flow condition. We examine the conditions under which the quasi-steady approximation of the glottal air-flow is valid. Influence of the time-varying flow on the location of the air-jet separation point is also investigated. To tackle this problem, a physical model of the vocal folds was constructed based on the standard M5 geometry (Scherer *et al.*, 2001). The time-varying flow condition was realized by sinusoidally modulating the flow rate with a frequency of 2 and 10 Hz. A theoretical model based on the boundary layer theory is further simulated to elucidate our experimental measurements.

The present paper is organized as follows. Section II describes the experimental methods. Our experimental set up as well as the vocal fold replica model is explained in detail. A theoretical model is also introduced here. Section III presents experimental as well as simulation results. Section IV is devoted to conclusions and discussions on the influence of time-varying flow on the intraglottal pressure profiles as well as on the vocal fold oscillations.

II. METHODS

A. M5 vocal fold model

Based on the M5 geometry of Scherer *et al.* (2001), an acrylic replica model of the vocal fold has been fabricated and used for the experiment. As shown in Fig. 1(a), the vocal fold replica represents an upscaled structure (7.5 times) of the human hemilarynx. The glottal entrance and exit are indicated on the lower and upper sides, respectively. As shown in Fig. 1(b), the left and right vocal folds were set to a symmetric and oblique configuration with a divergence angle of 5° and 5° (specifically, the angle Ψ, indicated in Fig. 1 of Scherer *et al.* (2001), was set to zero and the left and right vocal fold models were tilted by 5° clockwise and

counterclockwise, respectively). The airstream goes along the x axis (dorsoventral direction). The channel height $h(x)$ is defined on the y axis (mediolateral direction), where its minimum represents the aperture h_0. After the set-up of the left and right vocal folds, the aperture was measured at ten points uniformly located along the glottal length. At each point, a stack of feeler gages was placed through the glottis. As summarized in Fig. 1(c), the averaged aperture was $h_0 = 0.375 \pm 0.005$ mm. This aperture size was set in accordance with Scherer *et al.* (2001), who set h_0 to 0.4 mm.

On the vocal fold surface, 14 pressure taps were placed 2 mm apart from each other. They were staggered on either side of the centerline, which run along the airstream direction. The pressure taps were made flush and perpendicular to the vocal fold surface. The inner diameter of each pressure tap was 2 mm, while the diameter was narrowed to 0.3 mm at the vocal fold surface. In addition to the pressure taps on the vocal folds, another pressure tap was located upstream inside of the rectangular pipe, so as to measure the subglottal pressure as a reference. The 14 pressure taps were led to 14 pressure sensors (differential pressure transducer, DP15–28-N1S4A, Validyne Engineering, Northridge, CA; pressure amplifier PA501, KRONE Corporation, Tokyo, Japan) (flat response ranges between 25 and 36 Hz) *via* silicon tubing (tubing length of 40 cm). Another pressure sensor (Differential pressure transducer, PDS-70GA, Kyowa; Signal conditioner, CDV-700A, Kyowa, Tokyo, Japan) was used to monitor the subglottal pressure.

Prior to the experiment, the pressure sensors were calibrated using two liquid column manometers (MG 80, Sauermann; TJ 300, Sauermann, Montpon-Ménestérol, France). The sensors were labelled from $P1$ to $P15$ toward the downstream direction. $P1$ corresponds to the subglottal pressure ($x = 0$ [mm]), whereas $P15$ indicates the pressure at the supraglottal exit ($x = 59.8$[mm]). The location that corresponds to the aperture lies between $P7$ and $P8$.

B. Flow experiment

Intraglottal pressures were measured by injecting an airflow through the vocal fold model [see the experimental set–up of Fig. 1(d)]. To transfer an air-flow from air compressors (SilentAirCompressor SC820, Hitachi Koki, Tokyo, Japan; Rebicon 0.2LE-8SBA, Hitachi, Tokyo, Japan; UA 3810 A, Hikoki, Tokyo, Japan) to the vocal fold model, a long rectangular pipe (inner cross-sectional rectangular area: 0.08 m × 0.09 m, length: 2.8 m) was inserted between them [Fig. 1(f)].

The Reynolds number at the constriction is given by Re $= Uh_0/\nu$, where h_0 is the characteristic linear dimension of the flow channel (in this case, the aperture), $U = V/A_g$ is the average flow velocity in the minimum cross section area (V, volumetric flow rate; $A_g = h_0 l_g$, minimum area as a product of aperture and glottal width $l_g = 0.09$ m), and $\nu = 15 \cdot 10^{-6}$ m²/s is the kinematic viscosity of air. In the present steady flow experiment, the volumetric flow rate was varied from $V = 12$ l/min to $V = 53$ l/min. The corresponding
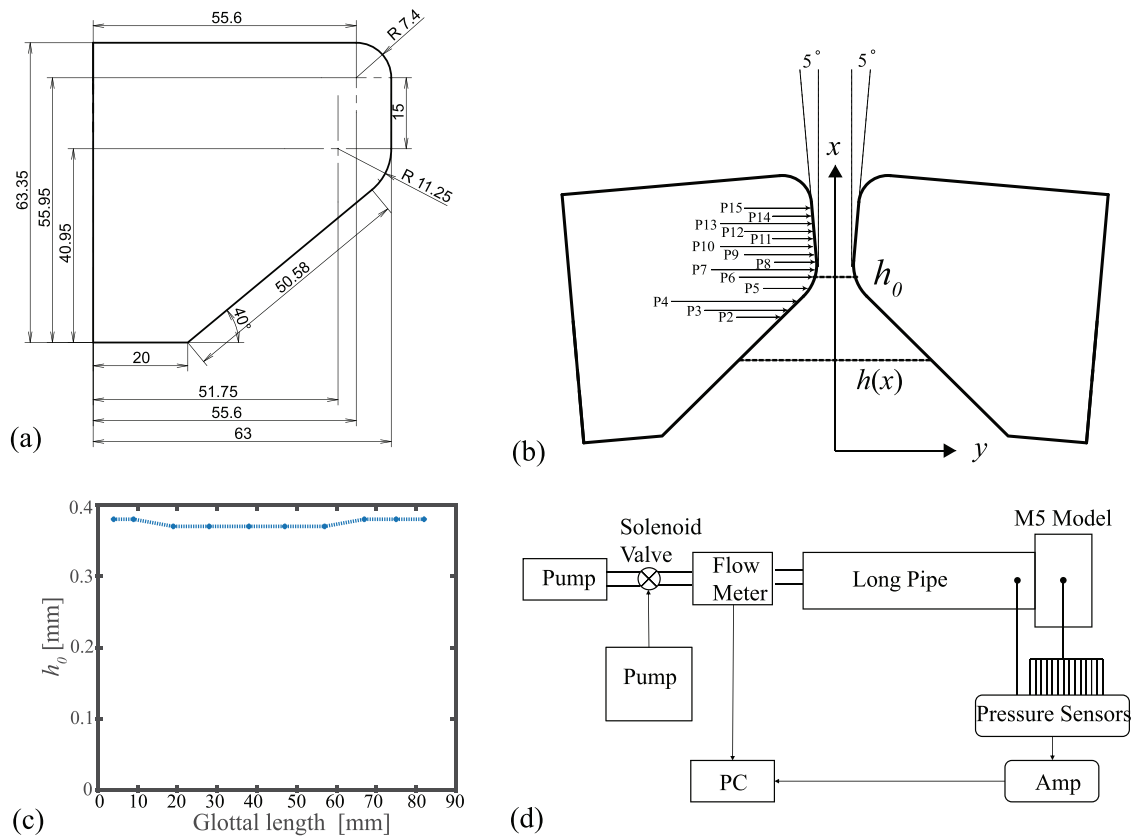
FIG. 1. (Color online) (a) Geometry and detailed dimensions [mm] of the M5 model. (b) Symmetric divergent configuration for the left and right vocal fold models. The left and right angles are set equally to 5° and 5°. The x- and y-axes are located towards dorsoventral and mediolateral directions. The airstream goes along the x-axis. The channel height $h(x)$ is defined on the y-axis, where its minimum represents the aperture h_0. Locations of the 14 pressure taps are indicated by the arrows. (c) Dependence of the aperture h_0 on the glottal location. (d) Experimental setup. Air-flow from the air compressors is regulated by the valve and the flow controller (or solenoid valve). It is then transferred to the vocal fold model through a long rectangular pipe. The subglottal pressure and the intraglottal pressures were measured simultaneously.

Reynolds number ranges from $\mathrm{Re} = 148$ to 654, that is in the range of laminar flows. According to Shah *et al.* (1978), the hydrodynamic entry length is given approximately as $l_h = 0.05 \cdot \mathrm{Re} \cdot D_h$ and, in our experiment, it ranges from 0.62 to 2.78 m [here, hydraulic diameter of the rectangular pipe is approximated as $D_h = 2 \cdot 0.08 \cdot 0.09/(0.08 + 0.09) = 0.085 \mathrm{m}$]. The pipe length of 2.8 m, used in the present set-up, covered most of the entry length D_h, which is required to reach to the fully developed flow.

For steady flow experiments, the flow rate from the air compressors was controlled by a pressure regulator (10202 U, Fairchild, Winston-Salem, NC) and a digital mass flow controller (CMQ–V, Azbil, Santa Clara, CA). For time-varying flow experiments, it was controlled by a solenoid valve (type 8605, Burkert; type 2873, Burkert, Ingelfingen, Germany) combined with a function generator (33500B Series, Keysight, Santa Rosa, CA). The volume flow rate was also monitored by a flow meter (Thermal Mass Flowmeters Series 4000, TSI, Shoreview, MN) (response time less than 4 ms).

For the steady flow experiment, the flow rate was varied from 12 l/ to 53 l/min with an increment of 1 l/min. For the time-varying flow experiment, the flow rate was sinusoidally modulated with a frequency of 2 Hz and 10 Hz by the solenoid valve and the function generator. All signals were stored in a digital recorder (Controller, PXIe-8840, National

Instruments; Input/output card, BNC-2110, National Instruments; Software, Labview, National Instruments, Tokyo, Japan) with a sampling frequency of 20 kHz.

According to the experimental study of measuring the intraglottal pressures (Scherer *et al.*, 2001), one side of the vocal fold forms a "flow-attached wall," while the other forms a "flow-detached wall." In the flow-attached wall, the flow is attached to the glottal surface until it separates near the glottal exit, whereas, in the flow-detached wall, the air-jet separation occurs further upstream in the glottis. In our experiments, they were detected manually by placing a hand in front of the vocal fold model to sense the flow direction. The direction of the glottal flow was switched by inserting a thin paper inside of the glottis and pulling it to the desired direction.

C. Theoretical model

To elucidate the steady-flow experiment, Thwaites boundary layer model was solved numerically (Deverge *et al.*, 2003; Hofmans, 1998). The theoretical model is based on the incompressible quasi-steady boundary layer theory. At moderate Reynolds numbers, viscous effects can indeed be assumed to be concentrated in a thin region, i.e., the boundary layer, near the walls of the channel (Schlichting and Gersten, 2016).

J. Acoust. Soc. Am. **151** (5), May 2022

Honda *et al.* 3131

Outside of the boundary layer, the flow is assumed to be inviscid and governed by Bernoulli's law together with the equation of mass conservation,

$$P(x) + \frac{1}{2}\rho v(x)^2 = P1, \qquad (1)$$

$$l_g\{h(x) - 2\delta^*(x)\}v(x) = const, \qquad (2)$$

where ρ is the air density, $v(x)$ the bulk velocity, and $\delta^*(x)$ is the displacement thickness of the boundary layer. Within the boundary layer, the two-dimensional viscous flow is described by the von Kármán equation, which is solved using the Thwaites method. Details about this resolution and validation against various glottal replicas can be found in Vilain et al. (2004).

Solving the boundary layer equation provides $\delta^*(x)$ in Eq. (2) and predicts the position of the air-jet separation point, for which the shear stress at the walls equals zero. The pressure profile $P(x)$ along the glottis can then be computed using Eq. (1).

III. RESULTS

A. Steady flow experiment

Figure 2 shows the results of the steady-flow experiment. Figures 2(a) and 2(b) indicate the pressure profiles under flow-detached wall condition, while Figs. 2(c) and 2(d) show those under flow-attached wall condition. Among 42 sets of measurements, five data sets corresponding to the volume-flow rate of 10 l/, 20 l/, 30 l/, 40 l/, and 50 l/min are plotted. Each curve shows that the pressure is high at the subglottis ($x = 0$ mm) and it rapidly drops near the glottal entrance ($x = 45.86$ mm), leading to a negative pressure. Then, the pressure recovers slowly to an atmospheric level. The air-jet separation point is located in this recovery process. Compared to the flow-attached wall condition, the pressure rise is faster in the flow-detached wall condition.

Following the work of Scherer et al. (2001), the air-jet separation point was defined as the point, where the pressure recovers to –5% of the subglottal pressure. Along the pressure curve, which was linearly interpolated from the discrete points measured by the sensors, the –5% point was identified. In each curve of Figs. 2(b) and 2(d), the air-jet separation point is indicated by a colored circle. This recovery point depends upon the flow rate. As the flow rate is increased, the recovery takes place in a more upstream region. Figure 2(e) shows dependence of the air-jet separation point on the subglottal pressure. The observed tendency is consistent with the earlier experimental and modelling studies on a round vocal fold shape (Cisonni et al., 2010, 2008; Scherer et al., 2001; Van Hirtum et al., 2009).

B. Theoretical model

To elucidate the steady-flow experiment, Thwaites boundary layer model was simulated. Figure 3 shows intraglottal pressure distributions of the boundary layer

model, in which the subglottal pressure was set to 29.5, 55.6, 170.3, and 286.1 Pa. The model curves (solid red lines) are compared with the experimental data (black error bars). To quantify the similarity between the model and the experiment, the glottal pressure forces, which act on the glottal surface, were calculated. The glottal forces in both x- and y-directions (x: dorsoventral direction; y: mediolateral direction) were integrated as $F_x = l_g \int_{x_1}^{x_2} (dh/dx)P(x)dx$ and $F_y = l_g \int_{x_1}^{x_2} P(x)dx$, respectively. Here, x_1 and x_2 determine the integration range, which were set to $x_1 = 10$ mm and $x_2 = 60$ mm. The model errors can be quantified as $e_\alpha = 100|F_\alpha^e - F_\alpha^m|/F_\alpha^e$ %, where the subscript α indicates x or y and the superscript indicates experiment (e) or model (m). Figure 3(e) shows the results. For 20 model simulations (the subglottal pressure ranges between 29.7 and 442.9 Pa), the modeling error was below 2% and 11% for the glottal forces F_x and F_y, respectively. For mathematical modeling of the vocal fold oscillations (Ishizaka and Flanagan, 1972; Pelorson et al., 1994; Steinecke and Herzel, 1995; Titze, 2000; Titze and Alipour, 2006), the 10% error may produce a certain mismatch, e.g., in phonation onset pressures, but it is within a tolerance range for simulation of a normal oscillation mode.

Finally, the model prediction of the air-jet separation point is compared with the experiment in Fig. 3(f). The model reproduced a qualitative feature of the experiment. Namely, in both model and experiments, the separation point moved towards an upstream region as the subglottal pressure was increased. Compared to the experimental curves, the model generally located the separation point in a more upstream region. The gap between the model and the flow-detached wall experiment ranged between –2 and –0.38 mm. In the sense that they are comparable to the distance between the pressure sensors (i.e., 2 mm), the model predicted the separation point within our experimental precision. As the subglottal pressure is increased to about 200 Pa, the gap decreases and reaches around 0.4 mm. Considering the simplified modeling assumptions, this level of agreement is considered good enough.

C. Time-varying flow experiment with 2 Hz

In the next experiments, time-varying flow was injected into the vocal fold model. Figure 4(a) shows two time traces of the subglottal pressure sinusoidally modulated with a frequency of 2 Hz. In the lower time trace, the subglottal pressure oscillated in the range between 51 and 278 Pa, whereas it oscillated in the range between 228 and 423 Pa in the upper time trace. Because of the long and large pipe, which prevents instantaneous transfer of the modulated air pressure at the solenoid valve to the subglottal area, there was a limitation in the oscillation range (227 and 195 Pa for lower and upper traces). Nevertheless, a combination of the two time traces covered a wide pressure range from 51 to 423 Pa. According to our manual detection of the flow direction at the glottal exit, the pressure profile measured by the sensors in these measurements was on the side of the flow-detached
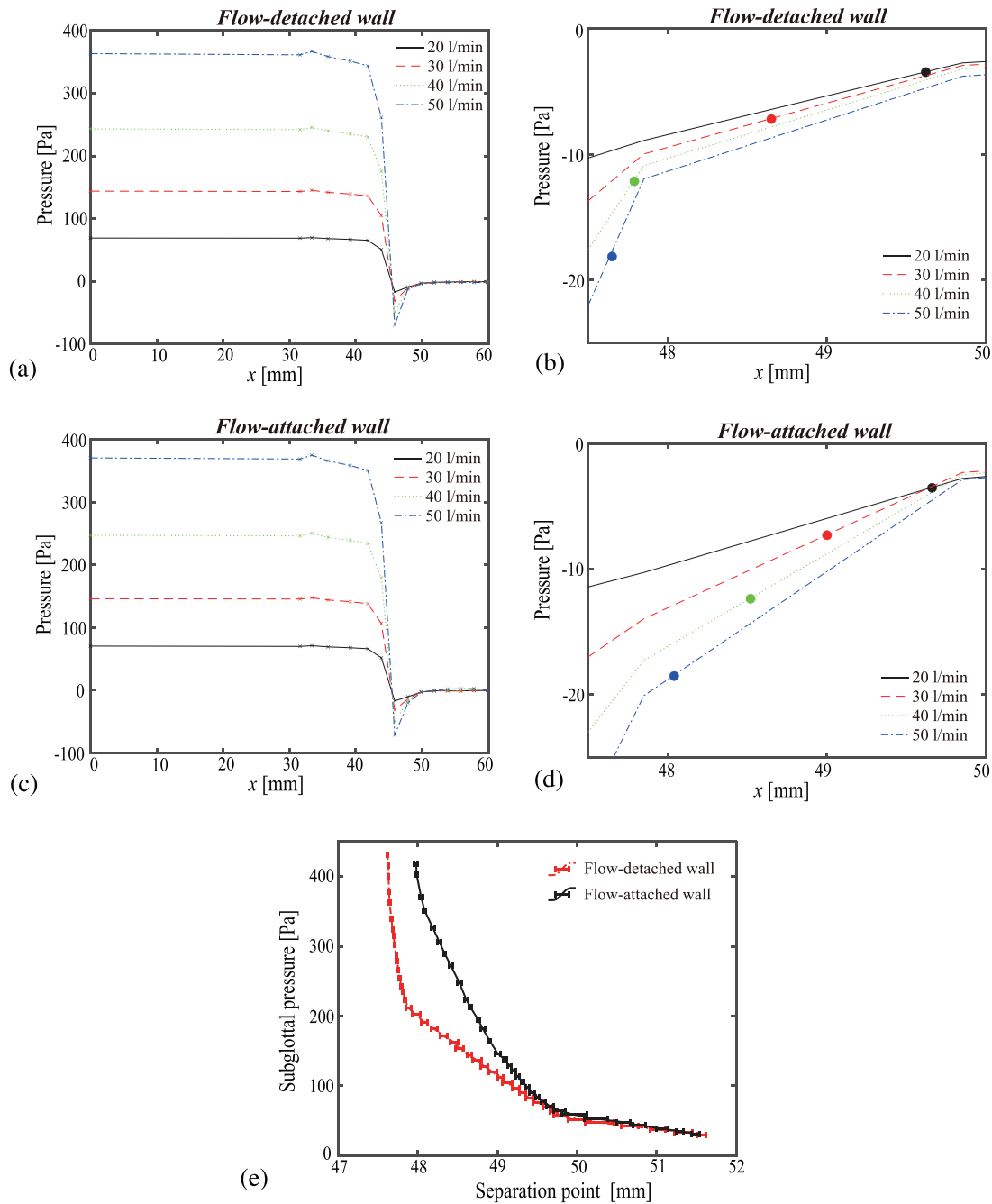
3132   J. Acoust. Soc. Am. **151** (5), May 2022

Honda et al.

FIG. 2. (Color online) Steady flow experiment. (a) Intraglottal pressure distribution (abscissa: x [mm], ordinate: pressure [Pa]) measured under *flow-detached wall* condition. The flow rate was varied as 10, 20, 30, 40, 50 l/min. (b) Enlarged graph of (a). The air-jet separation points (–5% level of the subglottal pressure) are indicated by circles. (c) Intraglottal pressure distribution (abscissa: x [mm], ordinate: pressure [Pa]) measured under *flow-attached wall* condition. The flow rate was varied as 10, 20, 30, 40, 50 l/min. (d) Enlarged graph of (c). (e) Dependence of the air-jet separation point on the subglottal pressure. The dotted red line and the solid black line correspond to the *flow-detached wall* and *flow-attached wall* conditons, respectively. The flow rate varied from 12 to 53 l/min with an increment of 1 l/min.

wall. By randomly selecting one point (red squares) in each time trace, the corresponding pressure profile was drawn. Figure 4(b) shows a snapshot of the pressure profile (dashed red line) observed at $t = 2.04$ s in the lower time trace (average and standard deviation of 50 consecutive points are indicated). The subglottal pressure was 171.0 ± 2.3 Pa. To compare this pressure profile with that under steady flow condition, steady flow data were selected in such a way that its subglottal pressure is located close to that of the time-

varying flow data. The pressure profile of the selected steady data, which had the subglottal pressure of 1701.0 ± 2.7 Pa, is drawn simultaneously in Fig. 4(b) (average and standard deviation of 50 consecutive points are indicated by the solid black line). The two pressure profiles were quite similar to each other. The t-tests indicated no pressure difference between the steady and time-varying flow conditions at taps P6 ($p = 0.051$), P7 ($p = 0.23$), and P8 ($p = 0.78$), where the separation point is located. Following the formula
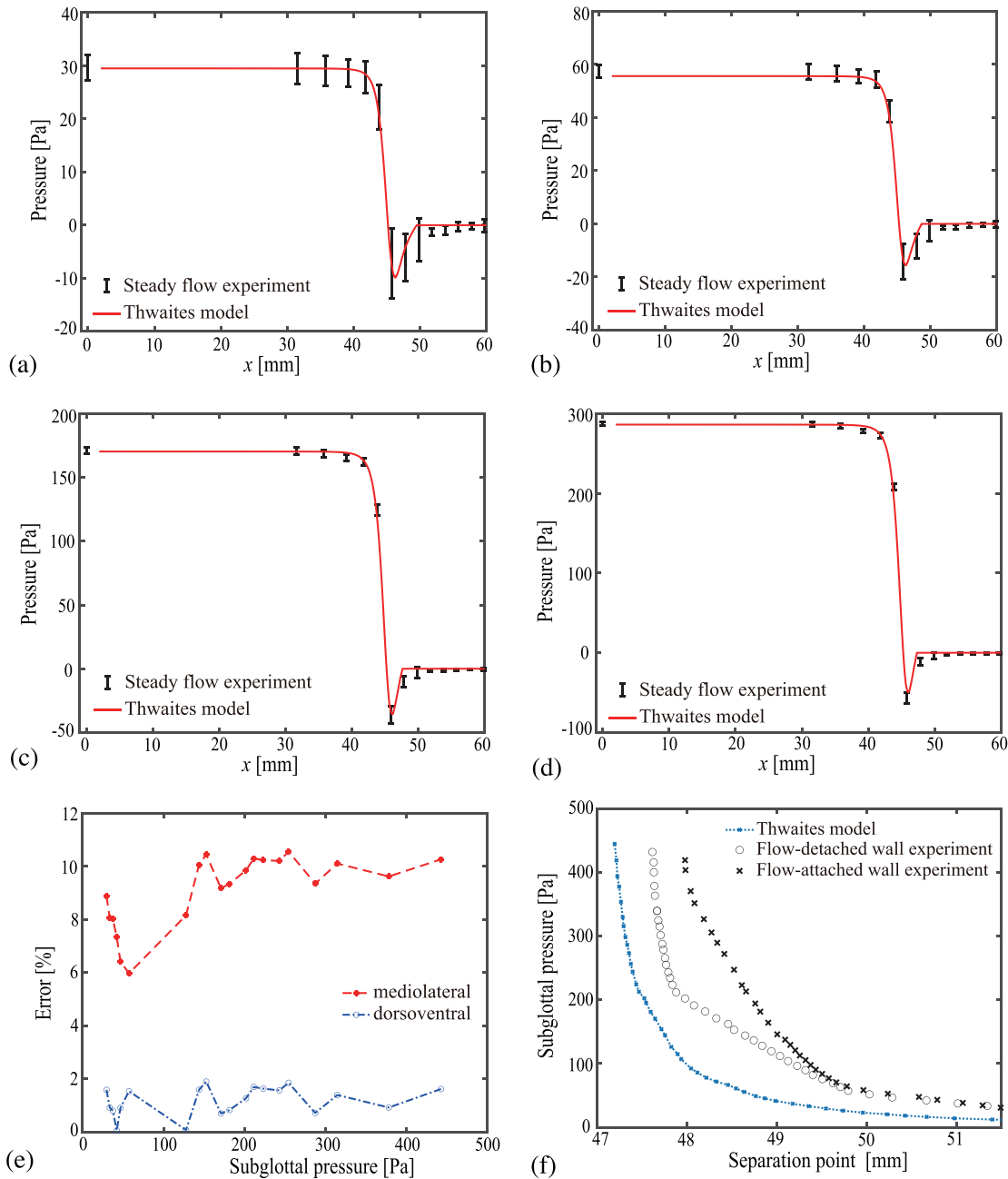
FIG. 3. (Color online) Simulation of Thwaites boundary layer model. (a)–(d) Simulated intraglottal pressure distributions (abscissa: x [mm], ordinate: pressure [Pa]) (solid red lines) are compared with the experiment (black error-bars). The subglottal pressure was set to 29.5, 55.6, 170.3, and 286.1 Pa in (a), (b), (c), and (d), respectively. (e) Dependence of the modeling errors, e_x (bule open circles) and e_y (red filled circles), on the subglottal pressure. The errors are defined as difference in the glottal pressure forces between the model and the experiment. (f) Dependence of the air-jet separation point on the subglottal pressure. The theoretical curve predicted by the Thwaites boundary layer model is drawn by blue asterisks, whereas the experimental data measured under flow-detached wall and flow-attached wall conditions are indicated by black circles and crosses.

introduced in Sec. III B, the glottal pressure forces were calculated as $(F_x, F_y) = (-0.472\,\text{N}, 0.513\,\text{N})$ and $(-0.476\,\text{N}, 0.518\,\text{N})$ for the steady and time-varying conditions, respectively. Their difference in the pressure forces were quite small ($e_x = 0.87\%$ and $e_y = 0.87\%$).

Figure 4(c) shows another snapshot of the pressure profile observed at $t = 2.04\,\text{s}$ in the upper time trace of Fig. 4(a). The time-varying flow data (subglottal pressure: $339.0 \pm 2.5\,\text{Pa}$) is compared with the closest steady flow data (subglottal pressure: $339.1 \pm 3.4\,\text{Pa}$). Again, the two

pressure profiles were not distinguished from each other (t-tests for P6: $p = 0.54$, P7: $p = 0.72$, P8: $p = 0.93$). The glottal pressure forces were $(F_x, F_y) = (-0.934\text{N}, 1.019\text{N})$ and $(-0.939\text{N}, 1.026\text{N})$ for the steady and time-varying flow conditions, respectively, with the errors of $e_x = 0.58\%$ and $e_y = 0.64\%$.

To confirm that these two points represent general property of the time-varying flow data, other data points were further examined. Namely, 200 time points were randomly selected from the time-varying data and the same comparisons
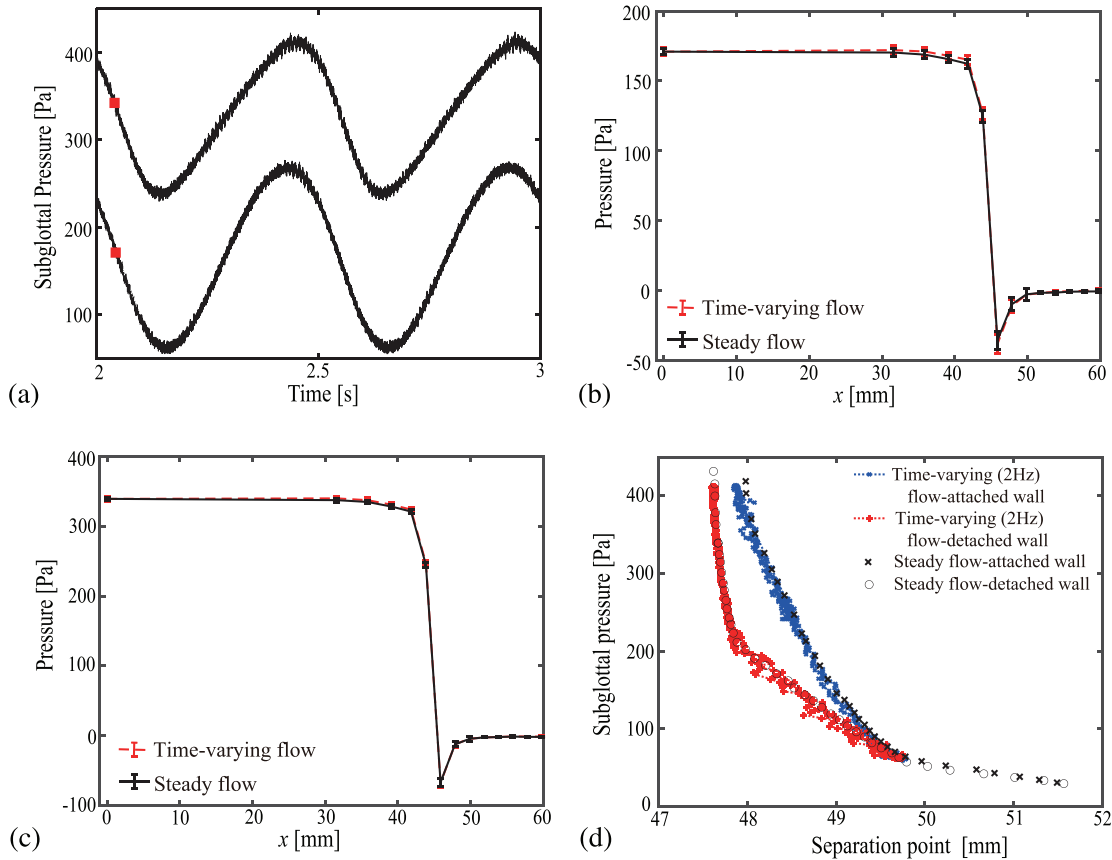
FIG. 4. (Color online) Experiment of time-varying flow sinusoidally modulated with a frequency of 2 Hz. (a) Time traces of the subglottal pressure which varied in the ranges between 51 and 278 Pa and between 228 and 423 Pa. (b) Intraglottal pressure distribution (abscissa: x [mm], ordinate: pressure [Pa]) (dashed red line) measured when the subglottal pressure was $P_s = 171.0 \pm 2.3$ Pa [red square in (a)]. For comparison, pressure distribution (solid black line) measured under steady flow (subglottal pressure: $P_s = 171.0 \pm 2.7$ Pa) is also drawn. (c): Intraglottal pressure distribution (dashed red line) measured when the subglottal pressure was $P_s = 339.0 \pm 2.5$ Pa [red square in (a)]. For comparison, pressure distribution (solid black line) measured under steady flow (subglottal pressure: $P_s = 339.1 \pm 3.4$ Pa) is also drawn. (d) Dependence of the air-jet separation point on the subglottal pressure. The red plus signs and the blue crosses correspond to the results estimated from the flow-detached wall and flow-attached wall data, respectively. The results estimated under steady flow are drawn in black circles and crosses.

were made. No difference was detected for 185 pairs of steady and time-varying flow data (significance level of $\alpha = 0.05$), while a slight difference was detected only for 15 pairs. The averaged difference in the glottal pressure forces was less than 1% (i.e., $e_x = 0.68 \pm 0.67\%$, $e_y = 0.73 \pm 0.73\%$). This implies that the pressure profiles of the time-varying flow data are non-distinguishable from the steady flow data as far as they have the same subglottal pressure as an input pressure. Thus, the time-varying flow can be viewed as a series of steady flow states with a time-varying subglottal pressure.

For the flow-attached wall data, similar results have been obtained. Among 200 pairs of steady and time-varying flow data, 188 pairs indicated no significant difference in their pressure profiles. The averaged difference in the glottal pressure forces was less than 1% (i.e., $e_x = 0.69 \pm 0.63\%$, $e_y = 0.75 \pm 0.74\%$).

To demonstrate that detailed information on the steady flow is contained in a short time window of the time-varying flow, the air-jet separation points were detected from the snapshots of the time-varying flow data and drawn as a function of the subglottal pressure in Fig. 4(d). The red plus signs and the blue crosses correspond to the results

estimated from the flow-detached wall and the flow-attached wall data, respectively. They are in good agreement with the steady flow data indicated with black circles and black crosses, implying that movement of the separation point in the time-varying flow can be well predicted by the steady flow data. As shown in Appendix, the oscillation frequency of 2 Hz corresponds to 112.5 Hz in real life, which is in the range of a typical male vocalization (Huber *et al.*, 1999).

D. Time-varying flow experiment with 10 Hz

To examine whether the previous results on the time-varying flow experiment can be extended to a higher forcing frequency, we have increased the forcing frequency to 10 Hz and measured the time-varying pressure distribution inside the glottis. Because of the limited capability of the flow controller, the oscillation amplitude of the subglottal pressure became smaller (32.0 ± 1.6 Pa). To cover a wide pressure range, 15 sets of pressure waveforms were produced, covering the total range from 46.6 to 370.8 Pa. In these experiments, the flow direction at the glottal exit indicated that the pressure taps were on the side of the flow-detached wall.

Figure 5(a) shows five time traces of the subglottal pressure sinusoidally modulated with a frequency of 10 Hz. Each time trace covers a different range of the pressure.

Figure 5(b) shows a snapshot of the pressure profile observed at $t = 0.074$ s [red square point indicated in the second time trace from the bottom in Fig. 5(a)]. The subglottal pressure was $P_s = 181.9 \pm 2.2$ Pa. To compare with the steady flow condition, the steady flow data having a similar subglottal pressure of 181.9 ± 2.4 Pa was chosen and its pressure profile was drawn simultaneously. The two pressure profiles were quite similar to each other (t-tests for P6: $p = 0.56$, P7: $p = 0.58$, P8: $p = 0.40$). Their differences in the glottal pressure forces were less than 1% ($e_x = 0.50\%$, $e_y = 0.58\%$). In Fig. 5(c), the same comparison was made for another pressure profile observed at $t = 0.259$ s [red square point indicated in the upper time trace in Fig. 5(a)]. Again, the pressure profile of the time-varying flow (subglottal pressure: 264.8 ± 2.9 Pa) was not distinguished from that of the steady flow (subglottal pressure: 264.8 ± 2.4 Pa) by the t-tests (P6: $p = 0.29$, P7: $p = 0.50$, P8: $p = 0.70$). Their differences in the glottal pressure forces were tiny ($e_x = 0.01\%$, $e_y = 0.02\%$).

Next, for 300 time points randomly selected from the 15 time traces of the time-varying flow data, the corresponding steady flow data, which showed the closest subglottal pressure, were searched. Among such 300 pairs of steady and time-varying flow data, their pressure profiles were compared. For 264 pairs, no significant difference was detected (significance level of $\alpha = 0.05$). The averaged differences in the glottal pressure forces were less than 1% (i.e., $e_x = 0.70 \pm 0.74\%$, $e_y = 0.65 \pm 0.70\%$).

Similar results were obtained also for the flow-attached wall data. Among 300 pairs of steady and time-varying flow data, 267 pairs indicated no significant difference in their pressure profiles. Their differences in the pressure forces were again less than 1% (i.e., $e_x = 0.65 \pm 0.70\%$, $e_y = 0.67 \pm 0.72\%$).

Finally, the air-jet separation points were detected from the snapshots of the time-varying flow data and drawn as a function of the subglottal pressure in Fig. 5(d). The red plus signs and the blue crosses correspond to the results estimated from the flow-detached wall and the flow-attached wall data, respectively. They agree quite well with the steady flow data (black circles and black crosses). This implies that our view of approximating the time-varying flow as a series of steady flow
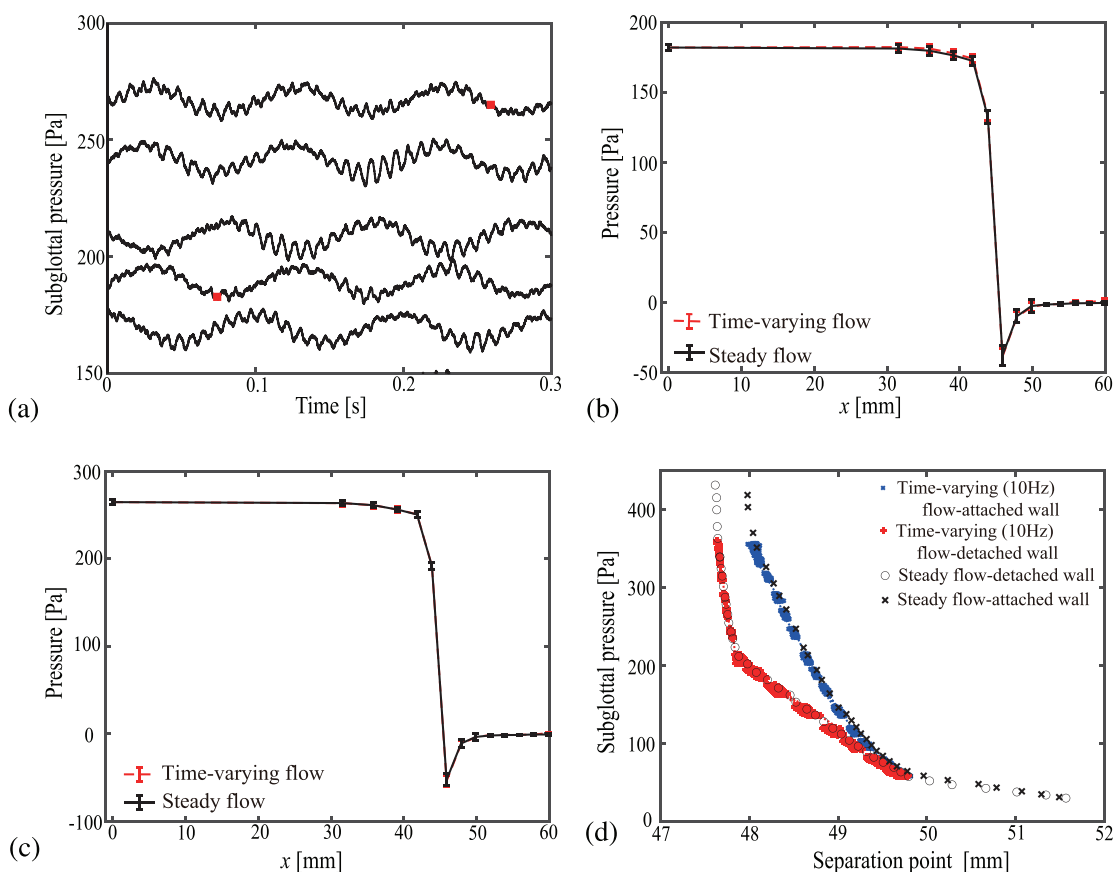

FIG. 5. (Color online) Results of time-varying flow, which was sinusoidally modulated with a frequency of 10 Hz. (a) Five time traces of the subglottal pressure. Each trace covers a different range of pressure. (b) Intraglottal pressure distribution (abscissa: X [mm], ordinate: pressure [Pa]) (dashed red line) measured when the subglottal pressure was $P_s = 181.9 \pm 2.2$ Pa [red square in the second time trace from the bottom in (a)]. For comparison, pressure distribution (solid black line) measured under steady flow (subglottal pressure: $P_s = 181.9 \pm 2.4$ Pa) is drawn simultaneously. (c) Intraglottal pressure distribution (dashed red line) measured when the subglottal pressure was $P_s = 264.8 \pm 2.9$ Pa [red square in the upper trace of (a)]. For comparison, pressure distribution (solid black line) measured under steady flow (subglottal pressure: $P_s = 264.8 \pm 2.4$ Pa) is drawn simultaneously. (d) Dependence of the air-jet separation point on the subglottal pressure. The red plus signs and the blue crosses correspond to the results estimated from the flow-detached wall and flow-attached wall data, respectively. The results estimated under steady flow are drawn in black circles and crosses.

states is valid even up to the frequency of 10 Hz, which corresponds to 562.5 Hz in real life. This frequency covers most of the range of the human voice (adult male, average around 105 Hz; adult female, average around 220 Hz; child, average around 260 Hz), although human voice can sometimes exceed 1000 Hz (e.g., singer's voice, Lamarche *et al.*, 2010).

IV. CONCLUSIONS AND DISCUSSIONS

To examine quasi-steady property of the glottal air-flow, various experimental studies have been carried out using a physical model of the vocal folds. In real vocalization, unsteadiness of the glottal pressure may originate mainly from two sources: time-varying flow and vocal fold movement. The effect of the latter has been investigated by using a moving vocal fold model (Deverge *et al.*, 2003; Krane *et al.*, 2010; Mongeau *et al.*, 1997; Ringenberg *et al.*, 2021; Vilain *et al.*, 2004; Zhang *et al.*, 2002), whereas the effect of the former has been studied by using a static vocal fold model and a time-varying flow (Hofmans *et al.*, 2003; Vilain *et al.*, 2004). Our study is based on a static vocal fold model and a time-varying flow, where detailed pressure distributions have been measured inside the glottis. Based on the M5 geometry of Scherer *et al.* (2001), a replica model of the vocal folds was constructed with an enlarged scale (7.5 times of the human hemilarynx). The left and right vocal folds were set to be symmetric with a divergence angle of 5° and 5°. The aperture was set to be small (i.e., 0.375 ± 0.005 mm, a length comparable to the study of Scherer *et al.*, 2001). The time-varying flow condition was realized by sinusoidally modulating the input air-flow to the vocal fold model with a frequency of 2 and 10 Hz. In the enlarged model, 2 and 10 Hz correspond to 112.5 and 562.5 Hz, respectively, in real life, which covers most of the pitch range of the human voice. By comparing with the steady flow data measured with variable subglottal pressures, we have shown that the pressure profiles of the time-varying flow data cannot be distinguished from those of the steady flow data as far as they have the same subglottal pressure as an input pressure. This has been confirmed for a wide range of subglottal pressures (from 51 to 423 Pa for 2 Hz; from 47 to 371 Pa for 10 Hz) and for both flow-attached wall and flow-detached wall conditions. We have moreover shown that the air-jet separation points were also in good agreement between the steady and time-varying flows. Our study therefore suggests that the time-varying glottal flow can be approximated as a series of steady flow states with a time-varying subglottal pressure. This supports the quasi-steady approximation of the glottal flow widely employed in mathematical modeling of the vocal fold oscillations, where the air-jet separation point is determined by assuming a steady flow inside the glottis (Ishizaka and Flanagan, 1972; Pelorson *et al.*, 1994; Steinecke and Herzel, 1995; Titze, 2000; Titze and Alipour, 2006). It should be noted that our experiment did not consider the case, in which the left and right vocal folds are closed or nearly closed. Under such a critical situation, the glottal flow should become more complex and unsteady. Our argument on the validity of the quasi-steady approximation is therefore limited to the case, in which the vocal folds do not completely close. Compared to the related preceding studies, which monitored glottal pressure at a few points of a fixed vocal fold model and reported quasi-steadiness of the glottal flow (Hofmans *et al.*, 2003; Vilain *et al.*, 2004), the present study provided a glottal pressure distribution in a significantly improved spatial resolution and moreover located the air-jet separation point precisely. Another note is that, in our experiment, the separation point moved as the subglottal pressure changed in time. The size of its movement was however less than 5 mm, which corresponds to 0.67 mm in real life. This implies that the movement of the separation point that occurs during the real phonation should be caused mainly by the changing shape of the glottis.

Further studies are needed for a comprehensive understanding of the effect of time-varying flow on the glottal pressure. In the present study, the time-varying flow was produced by the solenoid valve, which had a limited power of the flow control. As the oscillation frequency was increased from 2 to 10 Hz, the oscillation amplitude of the subglottal pressure decreased and became relatively small at 10 Hz. Under small-amplitude oscillations, the effect of large time-variations in the flow may not be fully examined. A more efficient system is needed for flow regulation, which enables large-amplitude oscillations at a higher frequency. A simple way is to make the aperture smaller so that the subglottal pressure becomes more sensitive to the volume flow rate of the glottis. Such a system may detect the critical frequency, above which the effect of time-varying flow appears to influence the intraglottal pressures. Our future study may focus on finding the critical frequency with the adjusted aperture. The influence of the left-right asymmetry between the vocal folds as well as the glottal shape (e.g., convergent and divergent shapes) on the time-varying pressure profile should be also investigated.

APPENDIX

Here we show how the timescale of the enlarged vocal fold model is translated into that of the real-life. For the sake of simplicity, we consider here the equations of an incompressible fluid,

$$\vec{\nabla} \cdot \vec{v} = 0, \tag{A1}$$

$$\rho_0 \frac{\partial \vec{v}}{\partial t} + \rho_0 (\vec{v} \cdot \vec{\nabla})\vec{v} = \vec{\nabla} p + \mu_0 \vec{\nabla}^2 \vec{v}, \tag{A2}$$

where $p = p(t, x, y, z)$ and $\vec{v} = \vec{v}(t, x, y, z)$ are respectively the flow pressure and velocity, μ_0 the dynamic viscosity coefficient, ρ_0 the air density, and $\vec{\nabla}$ the gradient operator.

For dimensional analysis, we introduce the following dimensionless variables:

$$\vec{v}^* = \frac{\vec{v}}{v_0}, \quad p^* = \frac{p}{\rho_0 v_0^2}, \quad t^* = \frac{t}{t_0}, \quad x^* = \frac{x}{l_0},$$
$$y^* = \frac{y}{l_0}, \quad z^* = \frac{z}{l_0},$$

where v_0 is a flow characteristic (typical) value, l_0 a characteristic dimension of the flow channel, and t_0 a characteristic timescale. Equation (A2) can be rewritten as

$$Sr \frac{\partial \vec{v}^*}{\partial t^*} + (\vec{v}^* \cdot \vec{\nabla}^*)\vec{v}^* = \vec{\nabla}^* p^* + \frac{1}{Re} \vec{\nabla}^{*2} \vec{v}^*, \qquad (A3)$$

with $Sr = l_0/t_0 v_0$ and $Re = \rho_0 v_0 l_0/\mu_0$, which represent the Strouhal and Reynolds numbers, respectively. Because of the normalization, all terms in Eq. (A3) are now comparable with each other. The Strouhal number appears thus as an indicator of the importance of the inertial terms $[\rho_0(\partial \vec{v}/\partial t)]$ with respect to the convective ones $(\rho_0(\vec{v} \cdot \vec{\nabla})\vec{v})$. In the same way, the Reynolds number (or $1/Re$) measures the importance of the convective terms with respect to the viscous terms $(\mu_0 \vec{\nabla}^2 \vec{v})$. Now the relevance of using Sr and Re relies on a sensible choice of the characteristic values and thus on some knowledge about the flow. Concerning the flow through the glottis, viscous losses are mainly dependent on the aperture (h_0) of the glottis. The relevant Reynolds number is thus

$$Re = \frac{\rho_0 v_0 h_0}{\mu_0}.$$

For the Strouhal number, the typical timescale should be the period of oscillation ($1/f_o$, where f_o is the fundamental frequency of the oscillation) and the characteristic dimension should be the thickness of the glottis (d_0). Indeed, the time needed by the flow to pass through the glottis can be estimated by d_0/v_0 and must be compared with t_0. The relevant Strouhal number is thus

$$Sr = \frac{d_0}{t_0 v_0}.$$

Using an up-scaled (or down-scaled) replica makes sense as long as Re and Sr (i.e., the physical effects of viscosity and inertia) are kept constant. Thus, if the replica is upscaled by a factor of N, keeping the Reynolds number constant means that the velocity on the replica must be N times lower than that in real life (because h_0 is N times larger than that in real life). Concerning the Strouhal number, d_0 is N times larger than that in real life, v_0 is N times lower than that in real life, thus t_0 is a factor N^2 times larger than that in real life. This means that an oscillation of 1 Hz on the replica corresponds to N^2 Hz in real life.

Note that the same demonstration could be done considering compressibility, in which the Mach number ($Ma = v_0/c_0$, where c_0 is the speed of sound) would appear as an extra dimensionless term. This is because, for voicing, $v_0 \ll c_0$, the compressible effects are considered of second order.

Alipour, F., and Scherer, R. C. (**2004**). "Flow separation in a computational oscillating vocal fold model," J. Acoust. Soc. Am. **116**(3), 1710–1719.

Cisonni, J., Van Hirtum, A., Luo, X. Y., and Pelorson, X. (**2010**). "Experimental validation of quasi-one-dimensional and two-dimensional steady glottal flow models," Med. Biol. Eng. Comput. **48**(9), 903–910.

Cisonni, J., Van Hirtum, A., Pelorson, X., and Willems, J. (**2008**). "Theoretical simulation and experimental validation of inverse quasi-one-dimensional steady and unsteady glottal flow models," J. Acoust. Soc. Am. **124**(1), 535–545.

Deverge, M., Pelorson, X., Vilain, C., Lagrée, P.-Y., Chentouf, F., Willems, J., and Hirschberg, A. (**2003**). "Influence of collision on the flow through in-vitro rigid models of the vocal folds," J. Acoust. Soc. Am. **114**(6), 3354–3362.

Hofmans, G., Groot, G., Ranucci, M., Graziani, G., and Hirschberg, A. (**2003**). "Unsteady flow through in-vitro models of the glottis," J. Acoust. Soc. Am. **113**(3), 1658–1675.

Hofmans, G. C. J. (**1998**). "Vortex sound in confined flows," Ph.D. thesis, Eindhoven University of Technology, Eindhoven, the Netherlands.

Huber, J. E., Stathopoulos, E. T., Curione, G. M., Ash, T. A., and Johnson, K. (**1999**). "Formants of children, women, and men: The effects of vocal intensity variation," J. Acoust. Soc. Am. **106**(3), 1532–1542.

Ishizaka, K., and Flanagan, J. L. (**1972**). "Synthesis of voiced sounds from a two-mass model of the vocal cords," Bell Syst. Tech. J. **51**(6), 1233–1268.

Krane, M. H., Barry, M., and Wei, T. (**2010**). "Dynamics of temporal variations in phonatory flow," J. Acoust. Soc. Am. **128**(1), 372–383.

Kucinschi, B. R., Scherer, R. C., DeWitt, K. J., and Ng, T. T. (**2006**). "An experimental analysis of the pressures and flows within a driven mechanical model of phonation," J. Acoust. Soc. Am. **119**(5), 3011–3021.

Lamarche, A., Ternström, S., and Pabon, P. (**2010**). "The singer's voice range profile: Female professional opera soloists," J. Voice **24**(4), 410–426.

Li, S., Scherer, R. C., Wan, M., Wang, S., and Wu, H. (**2006**). "The effect of glottal angle on intraglottal pressure," J. Acoust. Soc. Am. **119**(1), 539–548.

Mongeau, L., Franchek, N., Coker, C. H., and Kubli, R. A. (**1997**). "Characteristics of a pulsating jet through a small modulated orifice, with application to voice production," J. Acoust. Soc. Am. **102**(2), 1121–1133.

Pelorson, X., Hirschberg, A., Van Hassel, R., Wijnands, A., and Aurégan, Y. (**1994**). "Theoretical and experimental study of quasisteady-flow separation within the glottis during phonation. application to a modified two-mass model," J. Acoust. Soc. Am. **96**(6), 3416–3431.

Ringenberg, H., Rogers, D., Wei, N., Krane, M., and Wei, T. (**2021**). "Phase-averaged and cycle-to-cycle analysis of jet dynamics in a scaled up vocal-fold model," J. Fluid Mech. **918**, A44.

Scherer, R. C., Shinwari, D., De Witt, K. J., Zhang, C., Kucinschi, B. R., and Afjeh, A. A. (**2001**). "Intraglottal pressure profiles for a symmetric and oblique glottis with a divergence angle of 10 degrees," J. Acoust. Soc. Am. **109**(4), 1616–1630.

Scherer, R. C., Shinwari, D., De Witt, K. J., Zhang, C., Kucinschi, B. R., and Afjeh, A. A. (**2002**). "Intraglottal pressure distributions for a symmetric and oblique glottis with a uniform duct (L)," J. Acoust. Soc. Am. **112**(4), 1253–1256.

Scherer, R. C., Torkaman, S., Kucinschi, B. R., and Afjeh, A. A. (**2010**). "Intraglottal pressures in a three-dimensional model with a non-rectangular glottal shape," J. Acoust. Soc. Am. **128**(2), 828–838.

Schlichting, H., and Gersten, K. (**2016**). *Boundary-Layer Theory* (Springer, New York).

Shah, R., and Bhatti, M. (**1978**). *Laminar Convective Heat Transfer in Ducts* (Academic Press, New York).

Steinecke, I., and Herzel, H. (**1995**). "Bifurcations in an asymmetric vocal-fold model," J. Acoust. Soc. Am. **97**(3), 1874–1884.

Titze, I. R. (**2000**). *Principles of Voice Production*, 2nd ed. (National Center for Voice and Speech, Iowa City, IA).

3138   J. Acoust. Soc. Am. **151** (5), May 2022

Honda *et al.*

Titze, I. R., and Alipour, F. (**2006**). *The Myoelastic Aerodynamic Theory of Phonation* (National Center for Voice and Speech, Iowa City, IA).

Van Hirtum, A., Cisonni, J., and Pelorson, X. (**2009**). "On quasi-steady laminar flow separation in the upper airways," Commun. Numer. Methods Eng. **25**(5), 447–461.

Vilain, C., Pelorson, X., Fraysse, C., Deverge, M., Hirschberg, A., and Willems, J. (**2004**). "Experimental validation of a quasi-steady theory for the flow through the glottis," J. Sound Vib. **276**(3–5), 475–490.

Zhang, Z., Mongeau, L., and Frankel, S. H. (**2002**). "Experimental verification of the quasi-steady approximation for aerodynamic sound generation by pulsating jets in tubes," J. Acoust. Soc. Am. **112**(4), 1652–1663.

J. Acoust. Soc. Am. **151** (5), May 2022

Honda *et al.*   3139